Geothermics 118 (2024) 102912

Contents lists available at ScienceDirect

Geothermics

journal homepage: www.elsevier.com/locate/geothermics

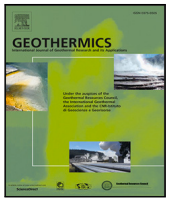

Exploiting heat gains along horizontal connection pipes in existing borehole heat exchanger fields

Stephan Düber [a,b,*], Raul Fuentes [a], Guillermo Narsilio [b]

[a] Institute of Geomechanics and Underground Technology, RWTH Aachen University, Aachen, Germany
[b] Department of Infrastructure Engineering, The University of Melbourne, Parkville, Australia

ARTICLE INFO

Keywords:
Borehole heat exchanger
Horizontal connection pipe
Header pipe
Heat loss
Heat gain
Optimised operation

ABSTRACT

This study investigates three options for utilising the additional capacity of borehole heat exchanger (BHE) fields through gains along horizontal connection pipes, whose contribution is routinely ignored. The analysis considers thermal load profiles with different heating to cooling ratios and finds that the effect of horizontal pipes becomes more significant with unbalanced loads. The study explores the potential of extended operation, increased loads and an optimised operating strategy to exploit the idle capacity gain from the horizontal connection pipes. It is shown that for the scenarios investigated, the BHE field operational time can be extended by more than 25 years without violating the critical fluid temperatures in the design phase. Alternatively, the thermal load can be increased by up to 26%. In addition, the study highlights the potential of an optimised operating strategy involving adjustments to the number of BHEs operated to reduce power consumption and therefore reducing operating costs in existing systems by utilising heat gains from the horizontal connection pipes.

1. Introduction

Apartment blocks, commercial buildings or entire neighbourhoods are increasingly being supplied with geothermal energy for heating and cooling. Shallow borehole heat exchangers (BHEs) with a typical depth of around 100 m are widely used in this context. Several BHEs are arranged in a borehole field to meet the energy needs of these large consumers. In Sweden alone the number of registered installations with 10 000 m or more total borehole length has almost quadrupled from 21 in 2015, to 76 systems in 2019, while the number of installations with 10 boreholes or more has increased by almost 40 % during the same period (Lund and Toth, 2021). To reduce the thermal interference in these borehole fields, a minimum distance between the individual boreholes should be maintained (VDI, 2019). Depending on the arrangement of the boreholes, significant distances of several dozen meters between the BHEs and manifolds, header pipes or the consumers must be bridged with horizontal connection pipes. While these pipes are typically buried at shallow depths without thermal insulation, their thermal interaction with the ground is usually not considered in the design (Kavanaugh and Rafferty, 2014; VDI, 2019). Research on horizontal pipes and BHEs is limited. However, modelling of heat transfer around buried pipes has been extensively studied in various contexts, including buried power cables, pipelines, district heating networks and, more recently, horizontal geothermal heat exchangers. Similar to the vertical boreholes (Li et al., 2016), a variety of analytical solutions exist based on the line or cylinder source theory utilising the method of images to take into account the ground surface (e.g. Ingersoll, 1948). The general solution for an arbitrarily oriented finite line source in a semi-infinite body was presented by Marcotte and Pasquier (2009). Following the work of Claesson and Javed (2011) and Cimmino and Bernier (2014) on vertical boreholes, Lamarche (2019) presented the general form for the segment-to-segment response for horizontal pipes, which eliminates the double integral in the work of Marcotte and Pasquier (2009). More recent works on horizontal ground heat exchangers also consider heat transfer mechanisms other than conduction using numerical models. The Piechowski (1999) finite difference model and the Gan (2019) finite volume model include mass transfer due to moisture content. The Gan (2013) finite volume model also includes freezing.

The effect of horizontal pipes in BHE installations has been studied only very briefly. Recent studies have examined the hydraulic effects of the connection pipes, but without in depth consideration of their thermal interference with the surrounding ground (Chen et al., 2020, 2021; Zhang et al., 2021). Luo et al. (2013) investigate the heat loss along a single buried pipe at different depths for flowing and stagnant fluid, and report the highest losses for stagnant fluid for heating operation in winter. Tian et al. (2022) investigate the effect of burial depth, surface temperature, backfill material and flow rate on the heat

* Corresponding author at: Institute of Geomechanics and Underground Technology, RWTH Aachen University, Aachen, Germany.
E-mail address: dueber@gut.rwth-aachen.de (S. Düber).

https://doi.org/10.1016/j.geothermics.2024.102912
Received 21 August 2023; Received in revised form 22 December 2023; Accepted 2 January 2024
Available online 9 January 2024

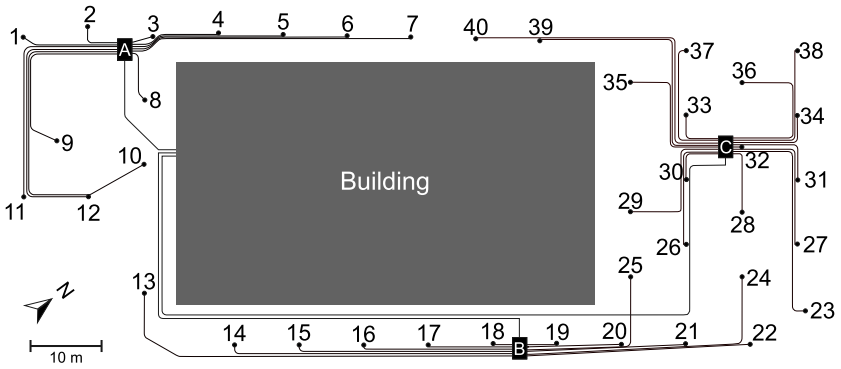

Fig. 1. Plan view of the connection pipe network of the 40 BHEs arranged in the three manifolds A, B and C.

loss of horizontal connection pipes attached to a BHE in a sandbox experiment. The whole system of heat pump, connection pipes and BHE under different climatic conditions is investigated by Düber et al. (2023). In contrast to the previous work, their study shows that the horizontal connection pipes have a positive effect in many applications, reducing the thermal load of the BHE and increasing the capacity of the whole system. They show that considering the connection pipes in the design can reduce the required depth of the vertical boreholes and therefore the cost.

In this work, we investigate how the extra capacity of connection pipes, not considered at the design stage, can be used in plants already in operation. Three optimisation options are investigated: *longer operation*, *higher loads* and an *optimised operating strategy* to reduce the electricity consumption of the heat and circulation pump. The study is based on a mixed-use university building in Germany, which is supplied with heating and cooling energy by 40 BHEs 100 m deep (Clauser et al., 2017).

In Section 2 we present a detailed description of the system of connection pipes and boreholes as well as the load profiles studied. Our modelling approach is presented in Section 3, where we first introduce the model for the connection pipes and BHEs, followed by our approach for the optimised operation strategy investigations. Finally, Section 4 presents the results and some discussions, followed by conclusions in Section 5.

2. Scenario

The study is based on the example of the EON.ERC building in Aachen, Germany. The building houses laboratories, conference rooms and offices. A field of 40 2U-type BHEs with a depth of 100 m supplies the building with heating and cooling energy. The BHEs are operated in parallel and are grouped into three manifolds A, B and C (Fig. 1). The connection pipes between the BHEs and the manifolds are buried at depths between 0.94 m and 1.54 m and are between 1.3 m (BHE 32) and 58.1 m (BHE 13) in length. The total length of all (supply and return pair of) connection pipes is 899 m, giving an average length per BHE of 22.5 m. This means that if the distance between the BHE and the manifold is 30 m, the length of the connecting pipe is here counted as 30 m, even though the supply and return pipe are each 30 m long. The properties of the BHEs, pipes and ground are listed in Table 1.

Fig. 2 shows the hourly ground thermal load of the BHE field over a one year period, derived from flow rates (measured with ultrasonic flow meter with ±2 % accuracy) and fluid temperatures (measured with Pt-1000s sensors with a limit deviation of $\pm 0.03 + 0.005|T|$ °C). The load is cooling dominant, with a cooling/heating ratio of 3.14. To introduce some variation representing other building types or use, we investigate 5 different load profiles with cooling/heating ratios between 0.1 and 10. We also perform the analysis with hourly load profiles as well as monthly averaged profiles, which are often used in engineering

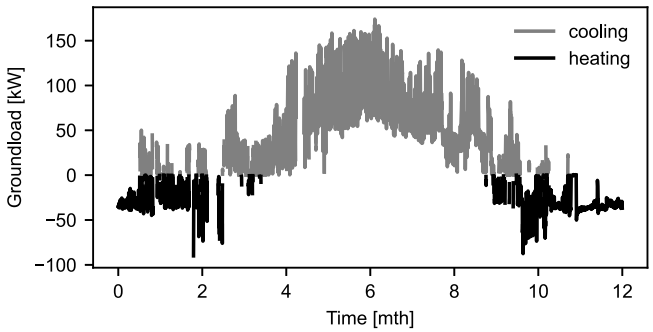

Fig. 2. Actual hourly ground load of the BHE field derived from measurements.

practice during the design phase. All load profiles are based on the profile shown in Fig. 2. To generate profiles with cooling/heating ratios of 0.1, 0.32, 1.0, 3.14 and 10, the measured profile is shifted towards heating or cooling until the desired ratio is reached. This is done by incrementally increasing or decreasing by 10 W all values not equal to 0 of the initial load profile with c/h = 3.14 until the desired c/h ratio is reached. It is then scaled as described in Düber et al. (2023) to meet the design criteria of the German technical guideline VDI 4640 (VDI, 2019), which states that for heating operation the BHE inlet temperature should not fall below 0 °C on a monthly average and should not fall below −5 °C at any time. In cooling mode, it should not exceed the undisturbed ground temperature by more than 15 °C on a monthly average and 20 °C at any time. The range of load ratios may represent different building uses and plants. Here, the g-function of the BHE field is calculated using the *pygfuntcion* toolbox (Cimmino and Cook, 2022) with the equal inlet temperature boundary condition and single segment BHEs which corresponds to our model as will be shown later in Section 3. The design period for the scaling of the load profiles is assumed to be 50 years. Fig. 3 shows all load profiles. To ensure that the monthly profiles have the same cooling/heating ratio as the hourly profiles, the profile in Fig. 2 was first averaged monthly and then shifted until the desired ratio was achieved.

When scaling the load profiles, the monthly average fluid temperature was the critical limit for all unbalanced load profiles. Only for the hourly profile with a cooling/heating ratio = 1.0 was the maximum fluid temperature during cooling the decisive limit. However, for the monthly averaged profile with the same ratio, it was again the monthly averaged fluid temperature, this time during heating operation.

3. Model and methods

We use the model recently introduced in Düber et al. (2023) for the system of BHEs and connection pipes. It is based on thermal resistances

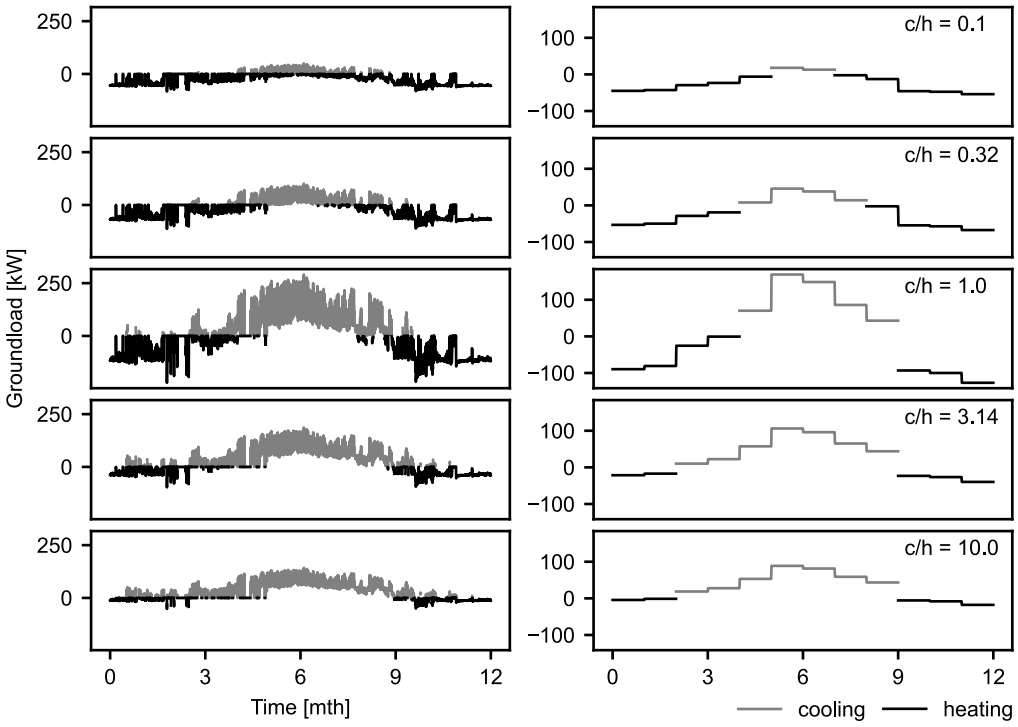

Fig. 3. Hourly (left) and monthly (right) load profiles with cooling/heating ratios (c/h) ranging from 0.1 to 10.

Table 1
BHE and ground properties of the BHE field (Clauser et al., 2017 and documents from the construction phase).

Domain	Parameter	Value	Units
Fluid	Thermal conductivity	0.43	$W\,m^{-1}\,K^{-1}$
Fluid	Density	1045	$kg\,m^{-3}$
Fluid	Volumetric heat capacity	3 800 000	$J\,m^{-3}\,K^{-1}$
Fluid	Dynamic Viscosity	0.0035	Pa s
Fluid	Flow rate per BHE	1.5	$m^3\,h^{-1}$
BHE	Length	100	m
BHE	Diameter	0.152	m
BHE	Shank space	0.04	m
BHE	Outer diameter pipes	0.032	m
BHE	Pipe wall thickness	0.0029	m
BHE	Thermal conductivity grout	2.0	$W\,m^{-1}\,K^{-1}$
BHE	Volumetric heat capacity grout	1 000 000	$J\,m^{-3}\,K^{-1}$
BHE	Thermal conductivity pipe	0.3	$W\,m^{-1}\,K^{-1}$
BHE	Borehole thermal resistance	0.089	$m\,K\,W^{-1}$
h. pipe	Length	1.3–58.1	m
h. pipe	Depth	0.94–1.54	m
h. pipe	Outer diameter	0.04	m
h. pipe	Wall thickness	0.0037	m
h. pipe	Thermal conductivity	0.38	$W\,m^{-1}\,K^{-1}$
h. pipe	Pipe thermal resistance	0.0989-0.0999	$m\,K\,W^{-1}$
Ground BHE	Thermal conductivity	2.3	$W\,m^{-1}\,K^{-1}$
Ground BHE	Volumetric heat capacity	2 300 000	$J\,m^{-3}\,K^{-1}$
Ground BHE	Undisturbed temperature	11.0	°C
Ground h. pipe	Thermal conductivity	2.0	$W\,m^{-1}\,K^{-1}$
Ground h. pipe	Volumetric heat capacity	2 000 000	$J\,m^{-3}\,K^{-1}$
Ground h. pipe	Undisturbed temperature	0.5–23.9	°C

for the pipes and BHEs and thermal response functions, also known as g-functions (Eskilson, 1987), for the ground around the BHEs and pipes. In the previous work we used the horizontal finite line source presented by Lamarche (2019) to calculate the g-functions for the horizontal pipes. Here, we use a 3D-numerical model to calculate the pipe g-functions. This allows us to take into account the different paths of the pipes as well as the impact of the building embedding into the ground (Fig. 1). For the sake of simplicity we make the following assumptions that differ from the actual conditions at the building: the ground surface is flat, the ground is homogeneous and the building is embedded 3 m into the ground over its entire footprint. To reduce the modelling effort, we neglect the thermal interference of horizontal pipes belonging to different manifolds. The minimum distance between connection pipes of different manifolds is about 10 m (BHE 23 and 24, see Fig. 1), while the maximum burial depth is 1.54 m. With this arrangement, the effects of mutual interference are dominated by the effects of the ground surface, even over long observation periods. This allows us to use individual models for each manifold, resulting in fewer elements and less computation for each model. The spatial discretisation of each model was verified with a grid independence test. Fig. 4 shows the

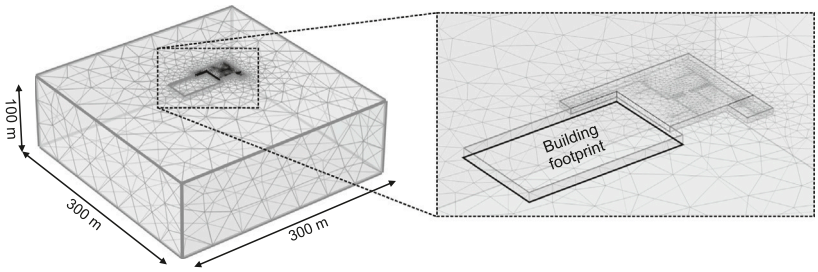

Fig. 4. Numerical model for calculation of g-functions for manifold C.

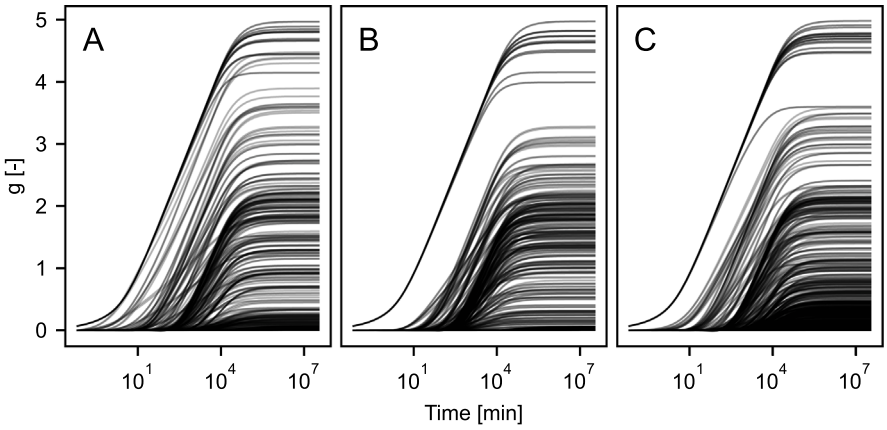

Fig. 5. G-functions for the horizontal pipes for manifolds A, B and C.

numerical model for manifold C. Since g-functions in essence capture changes in temperature (from the far-field or undisturbed ground temperature), rather that using the actual ground temperature, the initial temperature of the model is directly set to 0 °C. The boundaries of the model are set to have a constant temperature boundary condition of 0 °C. By choosing these values, the induced temperature change by heat injection along different pipes can be directly converted to the respective g-function without subtraction of undisturbed ground temperatures. Only the (boundary) faces where the building is embedded in the ground are considered to be thermally insulated (i.e., the portion of the upper boundary face with the building footprint). Considering supply and return pipe individually results in $(12 \cdot 2)^2 = 576$ g-functions for manifold A, $(12 \cdot 2)^2 = 576$ g-functions for manifold B and $(16 \cdot 2)^2 = 1024$ g-functions for manifold C (Fig. 5). Taking into account the $40^2 = 1600$ borehole g-functions adds up to a total number of 3776 g-functions considered in the model. The g-functions for the boreholes are calculated with the finite line source as presented by Claesson and Javed (2011).

The g-functions derived as described above serve as input parameters for the model presented in Düber et al. (2023). Here, the initial temperature at the BHEs is assumed to be constant as $T_{0,b} = 11$ °C. Unlike the common approach of considering a constant undisturbed ground temperature in vertical BHEs, the undisturbed ground temperatures for the horizontal pipes varies throughout the year and are calculated according to Phetteplace et al. (2013):

$$T_s(z,t) = T_{ave} + e^{-z\sqrt{\frac{\pi}{\alpha_s t_p}}} T_{amp} \sin\left[\frac{2\pi}{t_p}(t - \Phi) - z\sqrt{\frac{\pi}{\alpha_s t_p}}\right] \quad (1)$$

where T_{ave} is the average annual ground surface temperature, T_{amp} the amplitude of the ground surface temperature, t_p is the period of soil temperature cycle and t is the time. z is the depth at which the temperature is evaluated and α_s is the thermal diffusivity of the ground. The constants for Eq. (1) were derived from data from a nearby weather station as $T_{ave} = 12.2$ °C, $T_{amp} = 15.8$ °C and $\Phi = 106$ d. The resulting temperatures at the horizontal pipes are shown in Fig. 6.

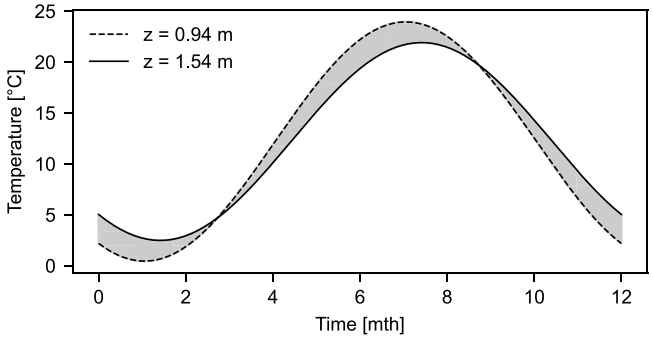

Fig. 6. Range of undisturbed ground temperatures at the horizontal connection pipes which are buried between 0.94 m and 1.54 m below the surface starting on the first of January.

The electricity consumers in a geothermal system are the circulation pump and the ground source heat pump. In Section 4.4 we assume active heating and cooling and try to reduce the total electricity demand with an optimised operating strategy. The idea is to not operate all BHEs at all times and therefore reduce the electricity demand of the circulation pump. This idea has already been explored by various authors outside the context of the horizontal connection pipes, partly in a modified form (e.g. Hackel and Pertzborn, 2011; Hecht-Méndez et al., 2013; Zarrella et al., 2017; Stoffel et al., 2022). While the investigations on longer operation time and higher loads (Sections 4.2 and 4.3) use the ground loads presented in the previous section, the analysis of an optimised operation strategy requires building loads and models for the heat pump and the circulation pump. Here, the ground load Q_g is calculated based on the building load Q_b, the temperature of the fluid exiting the BHE field and entering the heat pump $T_{in,HP}$ and the coefficient of performance (COP) of the heat pump. For cooling loads

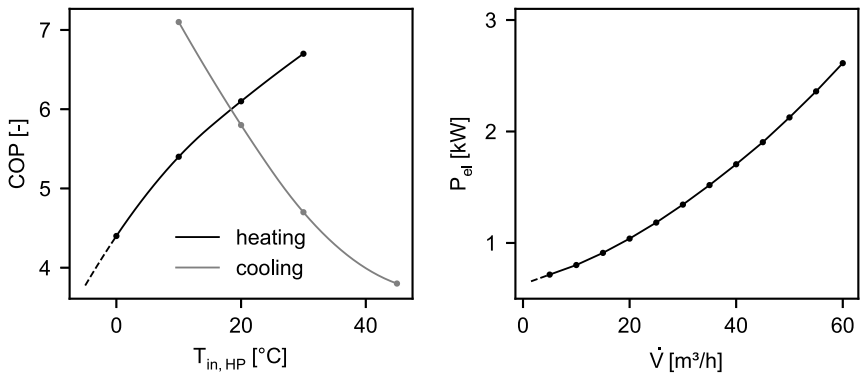

Fig. 7. Heat pump data (left) and circulation pump data (right) used for the model. Dashed lines indicate extrapolation.

we get:

$$Q_g = Q_b \frac{\mathrm{COP_c}(T_{\mathrm{in,HP}}) + 1}{\mathrm{COP_c}(T_{\mathrm{in,HP}})} \tag{2}$$

and for heating loads,

$$Q_g = Q_b \frac{\mathrm{COP_h}(T_{\mathrm{in,HP}}) - 1}{\mathrm{COP_h}(T_{\mathrm{in,HP}})}. \tag{3}$$

The COP is calculated based on manufacturer data (using Envision NKW150 as example only) shown in the left part of Fig. 7. For the inter- and extrapolation of the only pointwise available data we use the *scipy.interpolate.interp1d* function with a quadratic spline interpolater (Virtanen et al., 2020). To calculate the electricity consumption of the circulation pump, we use the same interpolation method on manufacturer data (using Wilo ChronoLine-IL-E 65 as example only) which is shown in the right part of Fig. 7. It is also assumed that all BHEs are hydraulically balanced and have a flow rate of $1.5\,\mathrm{m^3\,h^{-1}}$ regardless of the length of the individual connection pipe. It should be noted that the heat pump data shown in Fig. 7 does not correspond to the heat pump in the actual 20 yr old building, but to a contemporary GSHP, an assumption used here for our theoretical analysis.

For the optimised operating strategy, we divide the operating period of the BHE field into smaller periods of one month for which we want to determine the optimal number of BHEs in operation so that the electricity consumption is minimised. We have chosen an optimisation period of one month, or 12 control events per year, because the effort involved in switching the BHEs on and off seems justifiable, even if the task is undertaken manually without an automated control system or programmable BMS (building management system). To calculate the optimal number of BHEs for each period, we set up two models, a *simulation model* and a *prediction model*. The simulation model is the model already described, which is used for all analyses in this work. The predictor model is another instance of the same model, but with a coarser time step to reduce the computational effort.

The inputs for the predictor model are the average building load $\overline{Q}_b$ of the period and the temperatures at the boreholes T_{0b} and the horizontal pipes T_{0p}. The predictor model simulates the period for all cases from 1 to 40 BHEs in operation (i.e., using only 1, or only 2, or up to 40 BHEs at a time to satisfy the load in that period of time), using the described heat pump and circulation pump models. The optimal number of BHEs is selected based on the total electricity consumption P_{tot} and the critical fluid temperatures. This means that the number of BHEs is selected so that the critical fluid temperatures are maintained and the total power consumption is as low as possible. To ensure the most efficient selection of BHEs, the BHEs are first ordered according to their borehole wall temperatures. This depends on the average load of the period. If the load of the period is a building cooling load, the boreholes are sorted in ascending order starting with the coldest borehole, since it would have more capacity to reject heat to the ground than other BHEs. If it is a building heating load, the order is reversed and sorting starts with the warmest borehole. A flowchart of the described procedure is shown in Fig. 8.

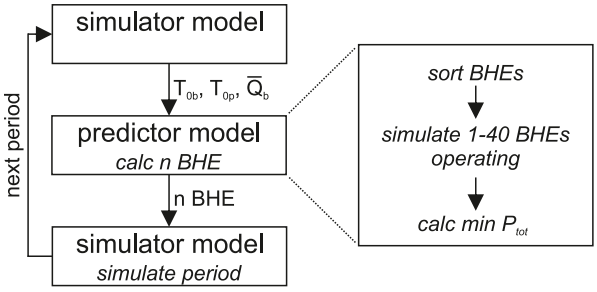

Fig. 8. Procedure to calculate the optimal number of BHEs operating for each period.

Fig. 9 shows the results of the predictor model for a period of heating operation. The bottom part shows the electricity consumption of the heat pump P_{HP}, the circulation pump P_{circ} and the sum of both P_{tot} as a function of the number of BHEs in operation.

The top part shows the corresponding inlet fluid temperature of the BHE field. As the number of BHEs increases, the power consumption of the circulation pump increases while the power consumption of the heat pump decreases, resulting in an overall optimum of 5 kW with 8 BHEs in operation. As the load for the period shown is a heating load, the fluid temperature increases as the number of BHEs increases. However, from 28 BHEs onwards we can see that it decreases slightly. This is due to the order of the BHEs. In the period prior to the current period of simulation, heating was also needed, and only 12 BHEs were in operation. By sorting the BHEs according to their borehole wall temperatures, these 12 BHEs are the least favourable for this period and are therefore only selected when 28 or more BHEs are required. Again, the optimum selection in terms of power consumption is 8 BHEs operating in this case.

To ensure comparability with the previous investigations on longer operation and higher loads (without heat pump model and ground load as boundary condition), the building loads are calculated so that the exact same ground loads occurs when using the heat pump model and building loads as boundary condition. Therefore we simulate the BHE field with 40 BHEs, including the connection pipes, with the specified ground loads (Fig. 3). Based on the fluid temperatures and the heat pump data (Fig. 7, left) we calculate the corresponding building load for each ground load profile.

4. Results and discussions

4.1. Effect of horizontal pipes

To give a first impression of the effect of the horizontal pipes, we simulate the BHE field at a constant cooling load of 120 kW for

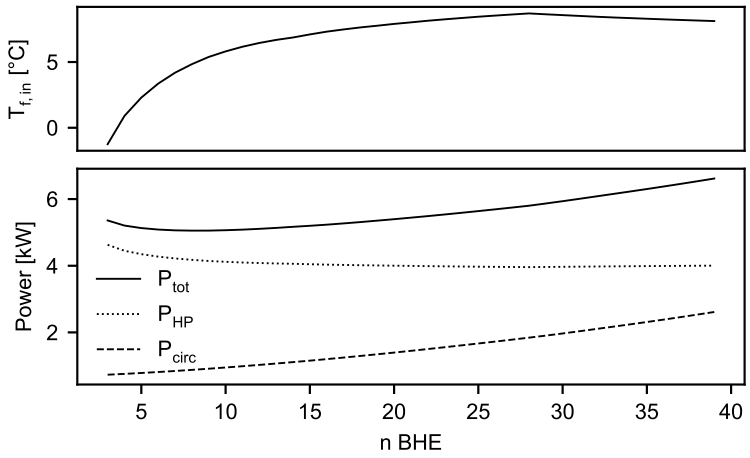

Fig. 9. Exemplary results of the predictor model.

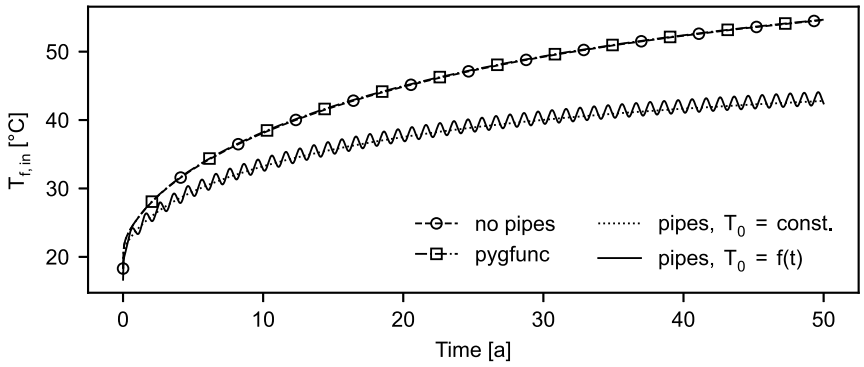

Fig. 10. Development of the fluid temperature entering the BHE field at a constant load of 120 kW with and without consideration of the horizontal connection pipes.

a period of 50 years. Fig. 10 shows the results for a simulation with our simulation model where the thermal conductivity of the horizontal pipes is set to zero (no pipes) and a simulation with the *pygfunction* toolbox as reference (pygfunc). Simulations with our model considering the pipes were performed with a constant undisturbed ground temperature around the pipes (pipes, T_0 = const.) and with varying ground temperatures (pipes, $T_0 = f(t)$).

The inclusion of the horizontal pipes leads to a difference in the fluid temperature entering the BHE field of more than 10 °C at the end of the period. The effect of the seasonal temperature variations around the horizontal pipes on the fluid temperature is rather small, resulting in a peak-to-peak amplitude of about 2 °C in this case. However, for the load profiles shown in Fig. 3, the effect of the horizontal pipes is less dramatic (Table 2). To demonstrate this, we simulate all scenarios with and without consideration of the horizontal pipes. Fig. 11 shows the results for the hourly load profile on the example of the c/h = 3.14 scenario where the temperature difference at peak loads is just 2 °C in the last year.

For the sake of clarity, we restrict the plots for all other cases to the envelopes of the fluid temperatures entering the BHE field. Fig. 12 shows the results for the hourly and monthly load profiles.

The results show that the more unbalanced the load profile, the greater the effect of the horizontal connection pipes (see also Tables 2 and 3). This is independent of whether the load profile is heating or cooling dominant. For unbalanced cooling-dominant profiles, the heat accumulates in the ground leading to a steady increase in fluid temperatures until eventually a steady state is reached. If the horizontal pipes are considered in the simulation, the capacity of the whole system is greater, leading to a slower temperature rise and possibly earlier reached state. The same applies to the heating loads, except that the ground is cooling instead of heating. Interestingly, in the case of balanced loads, the effect of the horizontal pipes is hardly noticeable. This is a special case that rarely occurs in practice.

Table 2
Average fluid inlet temperature [°C] of the BHE field for operational period of 50 years with and without consideration of the horizontal connection pipes.

c/h ratio	Hourly profile		Monthly profile	
	No pipes	Pipes	No pipes	Pipes
0.1	4.6	6.3	4.5	6.2
0.32	5.8	7.2	5.7	7.2
1.0	11.0	11.5	11.0	11.3
3.14	17.6	16.7	17.4	16.3
10.0	19.1	18.0	18.9	17.4

Table 3
Load share [%] covered by the BHEs for the different load profiles separated for cooling and heating operation.

c/h ratio	Hourly profile		Monthly profile	
	Heating	Cooling	Heating	Cooling
0.1	80.7	172.8	82.1	182.6
0.32	89.2	132.0	91.2	137.0
1.0	95.5	98.8	97.2	99.6
3.14	118.9	93.3	123.6	94.0
10.0	174.1	89.7	214.7	92.8

Table 2 shows the average fluid temperature entering the BHE field for the design period of 50 years with and without consideration of the horizontal pipes. The biggest difference with 1.7 °C occurs in the c/h = 0.1 scenario, both for hourly and monthly profiles, while the smallest effect can be observed for the balanced monthly profile (c/h = 1.0) with just 0.3 °C.

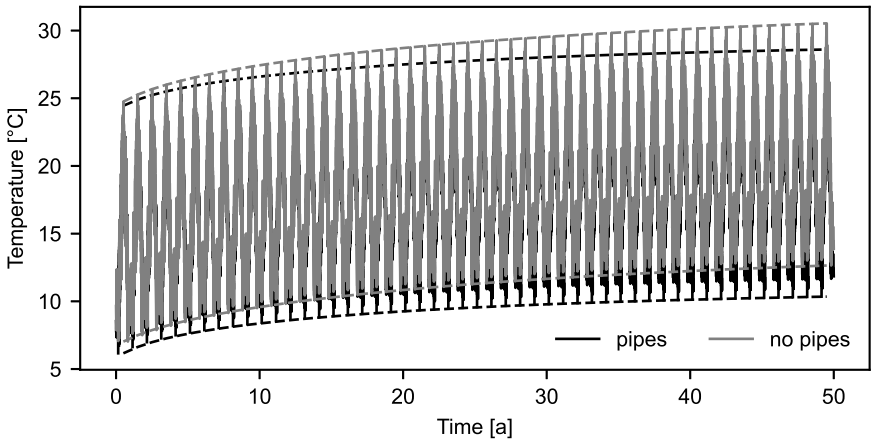

Fig. 11. Fluid temperatures entering the BHE field with and without consideration of the horizontal connection pipes for the c/h = 3.14 hourly load profile.

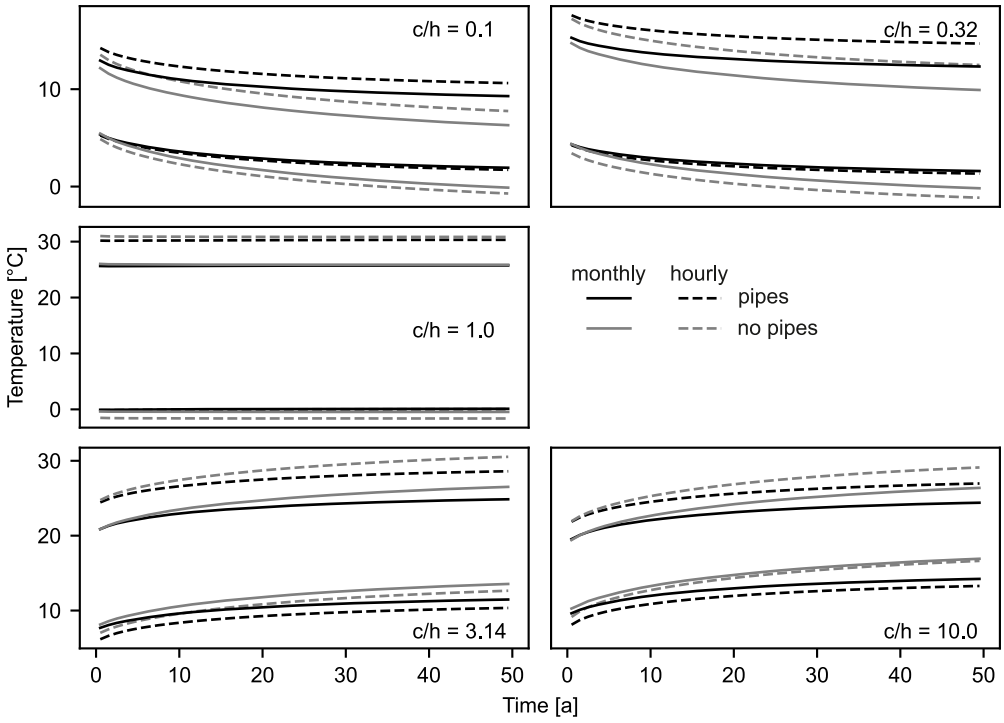

Fig. 12. Envelopes of the fluid temperatures entering the BHE field for all c/h ratios and monthly and hourly load profiles.

Table 3 shows the relative share of the load covered by the BHEs, taking into account the horizontal pipes. The dominant BHE thermal loads are reduced between 6 % (monthly profile, c/h = 3.14) and 19.3 % (hourly profile, c/h = 0.1). Load increases for the BHEs result exclusively for the non-dominant loads.

4.2. Longer operation

All load profiles have been scaled to reach the critical fluid inlet temperatures within the design period of 50 years, without consideration of the horizontal pipes. Based on technical guidelines, the BHE field can theoretically not be operated at the design loads after the 50-year period because the fluid temperatures will be either too high or too low. However, as shown in the previous section, the consideration of horizontal pipes leads to slower heat accumulation or depletion in the case of unbalanced load profiles. In this section we investigate how much longer the BHE field can operate with the same load profile by taking into account the horizontal connection pipes. Fig. 13 shows the results for the monthly profiles for an additional 25 years of operation or a total of 75 years of operation. Here, we plot the envelopes of the monthly averaged fluid temperatures entering the BHE field, as these were the decisive design criteria when scaling the loads (Section 2). Without the consideration of the pipes, the fluid temperatures reach the critical limit exactly after 50 years. Considering the pipes however, the fluid temperatures do not reach the critical limits even after 75 years for the same load profiles for all cases. In fact, the BHE field is almost in a steady state after this time, with negligible temperature accumulation. Fig. 14 shows the results for the hourly load profiles. The results are almost identical, only the absolute temperatures are slightly shifted.

4.3. Increased load

The increased capacity of the BHE field due to the consideration of the horizontal pipes will also allow higher loads within the same temperature limits. As our model only considers heat transfer through conduction, we can use the linear relation between temperature change

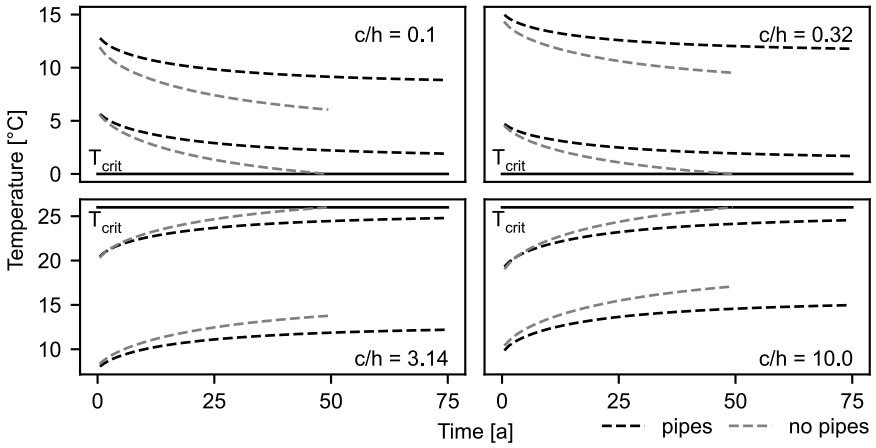

Fig. 13. Envelopes of the monthly averaged inlet temperature of the BHE field with and without consideration of the connection pipes for the monthly load profiles.

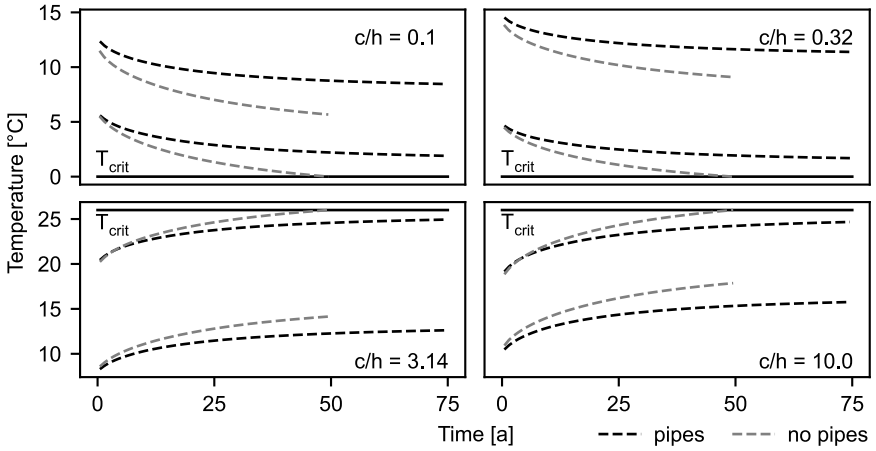

Fig. 14. Envelopes of the monthly averaged inlet temperature of the BHE field with and without consideration of the connection pipes for the hourly load profiles.

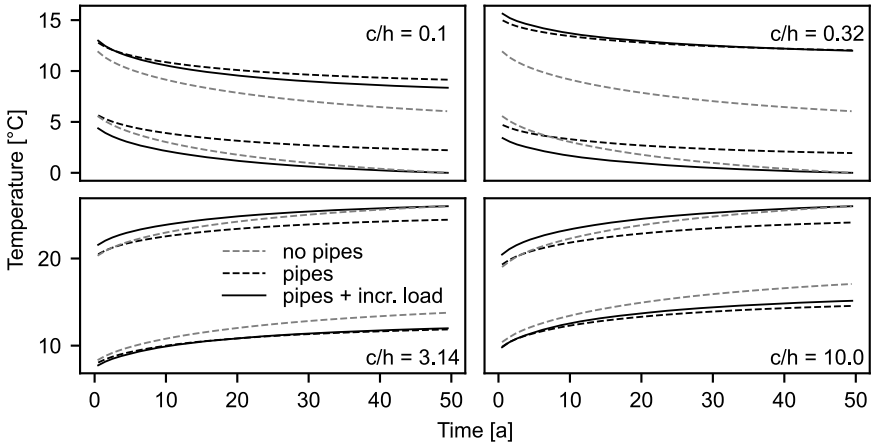

Fig. 15. Envelope of the monthly averaged fluid temperatures entering the BHE field for the monthly load profiles including the increased load profiles according to Table 4.

and thermal load to calculate the possible load increase directly. The results in Table 4 roughly coincide with the reduced BHE loads in Table 3, where the biggest reductions were observed for the unbalanced heating dominant profiles, followed by the unbalanced cooling dominant scenarios.

Fig. 15 shows an example of the results for the monthly load profiles. By considering the horizontal pipes, the load profile can be increased according to the factors in Table 4 so that at the end of the design period the exact same monthly average fluid temperatures are achieved as without considering the pipes.

4.4. Optimised operation

The previous sections have shown that neglecting the horizontal pipes in the design leads to an oversized system that allows for higher loads or longer operational times. In this section, we investigate

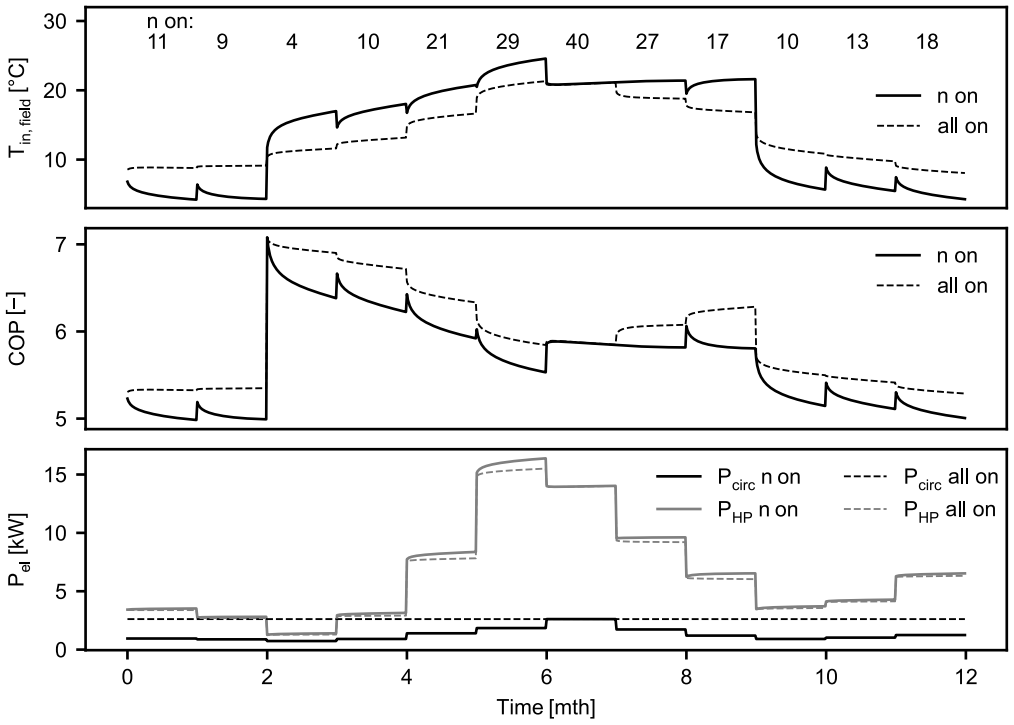

Fig. 16. Detailed results for the second year of the c/h = 3.14 case with monthly loads.

Table 4
Factors by which the load profiles can be multiplied until the critical fluid temperatures are reached considering the horizontal pipes.

c/h ratio	Hourly profile	Monthly profile
0.1	1.26	1.26
0.32	1.22	1.22
1.0	1.04	1.07
3.14	1.12	1.13
10.0	1.15	1.16

Table 5
Electricity savings with optimised operation strategy and the monthly load profiles.

c/h ratio	Electricity reduction %
0.1	17
0.32	12
1.0	3
3.14	11
10.0	15

whether the oversized system can be used more efficiently by applying an optimised operating strategy.

Fig. 16 shows detailed results for the second year of operation for the c/h = 3.14 case and the monthly load profile. The top part shows the fluid temperature entering the BHE field for the case with all BHEs operating and the optimal number of BHEs operating. The middle part shows the corresponding COP while the bottom part shows the electricity consumption of the heat and circulation pump. By not running all BHEs, the fluid temperatures decrease during heating (first two and last three months, see also Fig. 3) and increase during cooling. This results in a reduced COP of the heat pump and therefore increased electricity consumption, which is however compensated by the reduced electricity consumption of the circulation pump. For the period shown here the total electricity consumption if all BHEs are on at all times is 78 755 kW h while for the optimised number of BHEs operating it is just 69 211 kW h which corresponds to a reduction of 12 %.

For better clarity we limit the analysis for all cases and the full 50 year period to annual values as shown in Fig. 17. The left column shows the monthly averaged temperatures entering the BHE field of the month with the highest respectively lowest fluid temperature. The *no pipes* curves correspond to the scenario where the horizontal pipes are neglected, while the *pipes* curves show the fluid temperatures with consideration of the horizontal pipes. The *pipes, n on* curves finally show the fluid temperatures with some BHEs operating. The operation with less BHEs exploits the temperature reserve induced by the horizontal pipes, while staying within the temperature limits at all times. The right column of Fig. 17 shows the average annual electricity demand. The potential electricity savings are summarised in Table 5.

The proposed operating strategy works well with the monthly load profiles. The average monthly load used as input to the predictive model corresponds exactly to the load used later in the simulator model. Therefore, the predictive model is able to predict the fluid temperatures sufficiently accurately with significantly fewer calculation steps. However, applying the same approach to the hourly load profiles will result in temperature overshoots and even increased electricity consumption in some cases. Using a monthly average of the hourly load profile for the predictor model underestimates the BHE demand, especially when both heating and cooling loads are averaged. This is shown in the top part of Fig. 18 on the example of the c/h = 3.14 scenario.

The critical temperatures are particularly violated during the third month, where both heating and cooling loads occur (compare Fig. 3). Table 6 (a) summarises the results for all other c/h ratios. For the c/h = 1.0 scenario, the optimised operating strategy results even in an increased electricity consumption of 3 %, while the for the c/h = 10.0 scenario the critical fluid temperatures are violated during 14.1 % of the operational hours. In order to avoid underestimating the absolute loads by averaging heating and cooling loads within one month, we adjusted the input of the predictor model. Instead of using the average load of the whole month, we average heating and cooling loads within the month separately and use the dominant average as input for the predictor model. Exemplary results are shown in the bottom part of Fig. 18, note the increased number of BHEs operating most months.

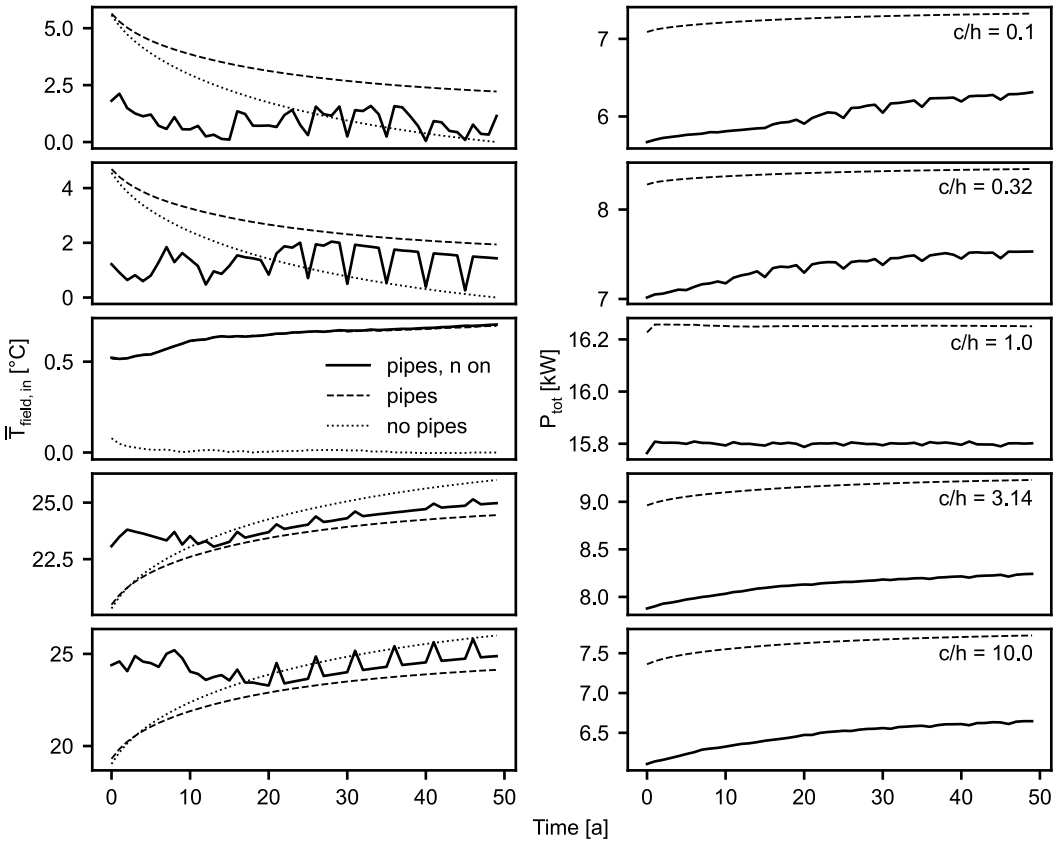

Fig. 17. Monthly averaged fluid inlet temperatures of the critical month (left) and total electricity consumption (right) for the monthly load profiles and the optimised operating strategy.

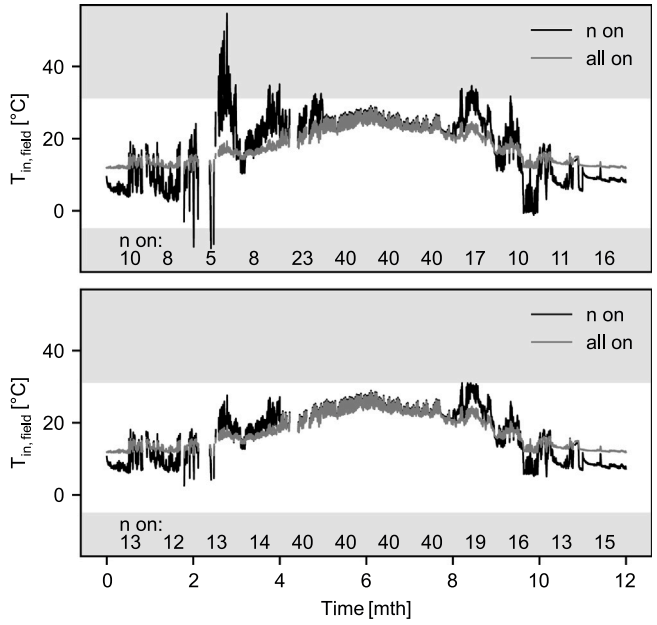

Fig. 18. Fluid inlet temperature of the BHE field for a one year period with all BHEs operating and the optimised operating strategy based on monthly averaged loads (top) and monthly averaged dominant loads (bottom). Range of critical fluid temperatures highlighted in grey.

The results listed under (b) in Table 6 show that the temperature constrain violations are greatly reduced and the electricity reduction is increased in most cases. In a final approach to prevent any temperature violations, we implemented a function in the simulation model, that activates two additional BHEs if 90 % of the critical fluid temperature is reached. The results are listed under (c) in Table 6. For the unbalanced load profiles, the temperature violations could be reduced by one order of magnitude with just 1–4 additional control events (switching on additional BHEs) per year, while for the balanced profile the number of control events almost doubled.

Fig. 19 finally shows the results for the hourly load profiles in the same way as in Fig. 17, here for the prediction based on the monthly average of the dominant load type (Table 6 (c)).

5. Conclusions

We investigated three ways to utilise the additional capacity of BHE fields due to the gains along horizontal connection pipes. The analysis with load profiles with different heating to cooling ratios showed that the more unbalanced the load profile, the greater the effect of the horizontal pipes. In fact, the effect of the pipes in combination with the perfectly balanced profile was almost negligible.

The German technical guideline VDI 4640 (VDI, 2019) requires that borehole heat exchangers are designed to ensure that the temperature of the fluid does not exceed certain limits during the operating period, which is typically 50 years. The investigations on longer operation revealed that even after 75 years of operation the critical temperatures were not reached for all scenarios, due to the additional gains along the connection pipes. Prolonging the (efficient) operation of existing BHE fields with a constant load profile is therefore a valid option to utilise the capacity gain from the connecting pipes.

Instead of extended operation, the thermal load can be increased (or conversely, the number of BHEs can be decreased in a new built situation). For the case c/h = 0.1, the load profile could be increased by 26 %, while for the case c/h = 1.0 it was only 4 %. The question here

Table 6
Electricity reduction [%], operating hours [%] in which the critical fluid temperatures were exceeded and average number of control events per year.

c/h ratio	Elect. reduction			Temp. violation			Control events		
	(a)	(b)	(c)	(a)	(b)	(c)	(a)	(b)	(c)
0.1	10	12	12	5.0	0.004	0.0	12	12	13
0.32	8	9	9	2.7	0.05	0.004	12	12	13
1.0	−3	2	2	7.2	0.4	0.009	12	12	23
3.14	9	9	13	2.3	0.15	0.003	12	12	15
10.0	11	13	13	14.1	0.1	0.001	12	12	16

(a) Prediction based on monthly average.
(b) Prediction based on monthly average of dominant load type.
(c) Prediction based on monthly average of dominant load type + additional control events.

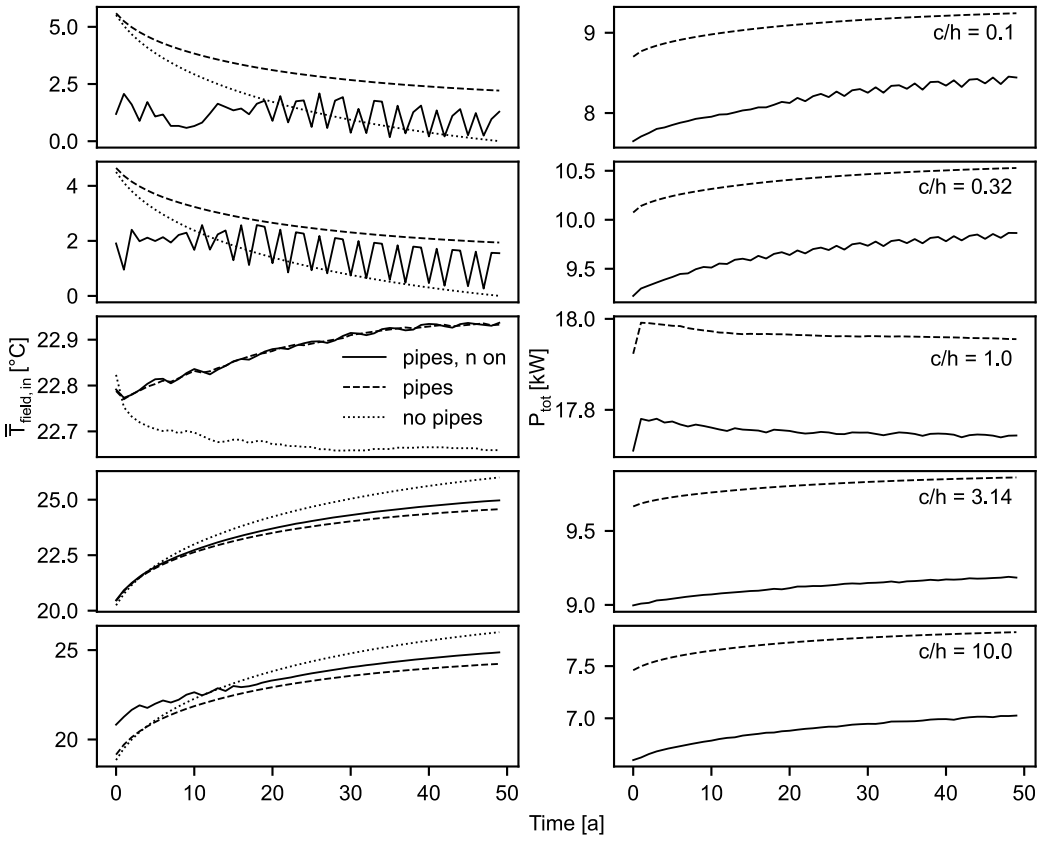

Fig. 19. Monthly averaged fluid inlet temperatures of the critical month (left) and total electricity consumption (right) for the hourly load profiles and the optimised operating strategy.

is to what extent this is possible in practice. With monovalent design, the BHE field is designed for the given building load, which is rather constant for many types of use and cannot be increased. If a BHE field is used mainly for cooling, the building loads may increase steadily due to climate change. In this case, the additional reserves provided by the connection pipes could ensure efficient operation. In a bivalent system, the share of geothermal energy can be increased according to the capacity reserve.

The investigations into the optimised operating strategy are based on the assumption that the number of BHEs operated and the flow rate of the circulation pump can be adjusted as required and that the energy demand for the optimisation period can be predicted with sufficient accuracy. By adjusting the number of BHEs operated on a monthly basis, the power demand could be reduced by up to 13 %. However, it was found that the critical fluid temperatures for the hourly load profiles were exceeded, but this occurred in less than 1 % of the operating hours. If the above conditions for an optimised operating strategy are met, it is a valid possibility to use the heat gains along the connection pipes to reduce operating costs in existing systems.

Finally, the results can be summarised as:

- Horizontal connection pipes (of considerable length) that were neglected in the design phase of a BHE field lead to additional heat exchange capacity.
- The effect of horizontal connecting lines is greatest with unbalanced load profiles, as the soil near the surface regenerates thermally more quickly.
- Unbalanced load profiles lead to temperature accumulation in the ground and at the BHE. This process is slowed down by taking the connecting pipes into account and the system can be operated in the intended temperature range for longer.
- The additional heat exchange along the connection pipes means that the thermal loads can be increased while maintaining the desired temperature range.
- The additional capacity due to the connection pipes theoretically leads to an oversized system. In this case, electrical energy can be saved under certain conditions by means of an optimised operating strategy.

As stated above, each of the investigated options has its requirements. The *longer operation* is most relevant for unbalanced load profiles with heat accumulation/depletion. The *higher loads* option is only applicable, if the actual loads can be adjusted, while the *optimised operation* requires control over individual BHEs and total flow rate as well as predictable loads. Under suitable boundary conditions, the options can also be combined as required.

CRediT authorship contribution statement

Stephan Düber: Conceptualization, Formal analysis, Investigation, Methodology, Software, Visualization, Writing – original draft. **Raul Fuentes:** Supervision, Writing – review & editing. **Guillermo Narsilio:** Supervision, Writing – review & editing.

Declaration of competing interest

The authors declare that they have no known competing financial interests or personal relationships that could have appeared to influence the work reported in this paper.

Data availability

Data will be made available on request.

Acknowledgment

This work was supported by the RWTH Aachen - University of Melbourne Joint PhD Program.

References

Chen, S., Cai, W.L., Witte, F., Wang, X.R., Wang, F.H., Kolditz, O., Shao, H.B., 2021. Long-term thermal imbalance in large borehole heat exchangers array - A numerical study based on the Leicester project. Energy Build. 231, http://dx.doi.org/10.1016/j.enbuild.2020.110518, ARTN 110518.

Chen, S., Witte, F., Kolditz, O., Shao, H.B., 2020. Shifted thermal extraction rates in large Borehole Heat Exchanger array - A numerical experiment. Appl. Therm. Eng. 167, http://dx.doi.org/10.1016/j.applthermaleng.2019.114750, ARTN 114750.

Cimmino, M., Bernier, M.A., 2014. A semi-analytical method to generate g-functions for geothermal bore fields. Int. J. Heat Mass Transfer 70, 641–650.

Cimmino, M., Cook, J.C., 2022. pygfunction 2.2 : New features and improvements in accuracy and computational efficiency. In: Spitler, J., Acuña, J., Bernier, M., Cimmino, M., Fang, Z., Gehlin, S., Javed, S., Liu, X., Rees, S., Stumpf, A. (Eds.), Research Conference Proceedings, IGSHPA Conference 2022. In: International Ground Source Heat Pump Association Annual Conference, International Ground Source Heat Pump Association, Las Vegas, pp. 45–52. http://dx.doi.org/10.22488/okstate.22.000015.

Claesson, J., Javed, S., 2011. An analytical method to calculate borehole fluid temperatures for time-scales from minutes to decades. ASHRAE Trans. 117, 279–288.

Clauser, C., Michalski, A., Müller, D., Fütterer, J., Stinner, F., 2017. Exergetisch optimierte Betriebsführung der Wärme- und Kälteversorgung eines Gebäudes unter Nutzung eines dynamischen Regelungssystems und flexibler Einbindung eines vollständig überwachten Erdwärmesondenfeldes : Endbericht. Technical Report, Institute for Energy Efficient Buildings and Indoor Climate, Aachen.

Düber, S., Fuentes, R., Narsilio, G., 2023. Effect of horizontal connection pipes on operation of borehole heat exchangers under different climatic conditions. Geothermics 110, 102679. http://dx.doi.org/10.1016/j.geothermics.2023.102679, URL: https://www.sciencedirect.com/science/article/pii/S0375650523000330.

Eskilson, P., 1987. Thermal Analysis of Heat Extraction Boreholes. (Ph. D. thesis). University of Lund, Lund, Sweden.

Gan, G., 2013. Dynamic thermal modelling of horizontal ground-source heat pumps. Int. J. Low-Carbon Technol. 8 (2), 95–105. http://dx.doi.org/10.1093/ijlct/ctt012.

Gan, G., 2019. A numerical methodology for comprehensive assessment of the dynamic thermal performance of horizontal ground heat exchangers. Therm. Sci. Eng. Prog. 11, 365–379. http://dx.doi.org/10.1016/j.tsep.2019.04.013.

Hackel, S., Pertzborn, A., 2011. Effective design and operation of hybrid ground-source heat pumps: Three case studies. Energy Build. 43 (12), 3497–3504. http://dx.doi.org/10.1016/j.enbuild.2011.09.014, https://www.sciencedirect.com/science/article/pii/S0378778811004026.

Hecht-Méndez, J., de Paly, M., Beck, M., Bayer, P., 2013. Optimization of energy extraction for vertical closed-loop geothermal systems considering groundwater flow. Energy Convers. Manage. 66, 1–10. http://dx.doi.org/10.1016/j.enconman.2012.09.019.

Ingersoll, L.R., 1948. Theory of the ground pipe heat source for the heat pump. Heat. Pip. Air Cond. 20, 119–122.

Kavanaugh, S.P., Rafferty, K.D., 2014. Geothermal Heating and Cooling: Design of Ground-Source Heat Pump Systems. ASHRAE.

Lamarche, L., 2019. Horizontal ground heat exchangers modelling. Appl. Therm. Eng. 155, 534–545. http://dx.doi.org/10.1016/j.applthermaleng.2019.04.006.

Li, M., Zhu, K., Fang, Z., 2016. Analytical methods for thermal analysis of vertical ground heat exchangers. In: Advances in Ground-Source Heat Pump Systems. pp. 157–183. http://dx.doi.org/10.1016/b978-0-08-100311-4.00006-6.

Lund, J.W., Toth, A.N., 2021. Direct utilization of geothermal energy 2020 worldwide review. Geothermics 90, http://dx.doi.org/10.1016/j.geothermics.2020.101915, ARTN 101915.

Luo, J., Rohn, J., Bayer, M., Priess, A., 2013. Modeling and experiments on energy loss in horizontal connecting pipe of vertical ground source heat pump system. Appl. Therm. Eng. 61 (2), 55–64. http://dx.doi.org/10.1016/j.applthermaleng.2013.07.022.

Marcotte, D., Pasquier, P., 2009. The effect of borehole inclination on fluid and ground temperature for GLHE systems. Geothermics 38 (4), 392–398. http://dx.doi.org/10.1016/j.geothermics.2009.06.001.

Phetteplace, G., Bahnfleth, D., Mildenstein, P., Overgaard, J., Rafferty, K., Wade, D., et al., 2013. District Heating Guide. ASHRAE, Atlanta.

Piechowski, M., 1999. Heat and mass transfer model of a ground heat exchanger: Theoretical development. Int. J. Energy Res. 23 (7), 571–588. http://dx.doi.org/10.1002/(Sici)1099-114x(19990610)23:7<571::Aid-Er462>3.0.Co;2-6.

Stoffel, P., Kümpel, A., Müller, D., 2022. Cloud-based optimal control of individual borehole heat exchangers in a geothermal field. J. Therm. Sci. 31 (5), 1253–1265. http://dx.doi.org/10.1007/s11630-022-1639-0, URL: https://publications.rwth-aachen.de/record/847450.

Tian, X., Mao, R., Pei, P., Wu, H., Ma, H., Hu, C., Zhang, Z., 2022. Experimental study on temperature control optimization of ground source heat pump horizontal headers. Energy Build. 277, http://dx.doi.org/10.1016/j.enbuild.2022.112541.

VDI, 2019. Thermal Use of the Underground - Ground Source Heat Pump Systems. VDI-Gesellschaft Energie und Umwelt.

Virtanen, P., Gommers, R., Oliphant, T.E., Haberland, M., Reddy, T., Cournapeau, D., Burovski, E., Peterson, P., Weckesser, W., Bright, J., van der Walt, S.J., Brett, M., Wilson, J., Millman, K.J., Mayorov, N., Nelson, A.R.J., Jones, E., Kern, R., Larson, E., Carey, C.J., Polat, İ., Feng, Y., Moore, E.W., VanderPlas, J., Laxalde, D., Perktold, J., Cimrman, R., Henriksen, I., Quintero, E.A., Harris, C.R., Archibald, A.M., Ribeiro, A.H., Pedregosa, F., van Mulbregt, P., SciPy 1.0 Contributors, 2020. SciPy 1.0: Fundamental Algorithms for Scientific Computing in Python. Nature Methods 17, 261–272. http://dx.doi.org/10.1038/s41592-019-0686-2.

Zarrella, A., Emmi, G., De Carli, M., 2017. A simulation-based analysis of variable flow pumping in ground source heat pump systems with different types of borehole heat exchangers: A case study. Energy Convers. Manage. 131, 135–150. http://dx.doi.org/10.1016/j.enconman.2016.10.061, https://www.sciencedirect.com/science/article/pii/S019689041630975X.

Zhang, M.F., Gong, G.C., Zeng, L.W., 2021. Investigation for a novel optimization design method of ground source heat pump based on hydraulic characteristics of buried pipe network. Appl. Therm. Eng. 182, http://dx.doi.org/10.1016/j.applthermaleng.2020.116069, ARTN 116069.